Original Article

T1 Measurements Identify Extracellular Volume Expansion in Hypertrophic Cardiomyopathy Sarcomere Mutation Carriers With and Without Left Ventricular Hypertrophy

Carolyn Y. Ho, MD; Siddique A. Abbasi, MD; Tomas G. Neilan, MD; Ravi V. Shah, MD;
Yucheng Chen, MD; Bobak Heydari, MD; Allison L. Cirino, MS, CGC; Neal K. Lakdawala, MD;
E. John Orav, PhD; Arantxa González, PhD; Begoña López, PhD; Javier Díez, MD, PhD;
Michael Jerosch-Herold, PhD; Raymond Y. Kwong, MD

Background—Myocardial fibrosis is a hallmark of hypertrophic cardiomyopathy (HCM) and a potential substrate for arrhythmias and heart failure. Sarcomere mutations seem to induce profibrotic changes before left ventricular hypertrophy (LVH) develops. To further evaluate these processes, we used cardiac magnetic resonance with T1 measurements on a genotyped HCM population to quantify myocardial extracellular volume (ECV).

Methods and Results—Sarcomere mutation carriers with LVH (G+/LVH+, n=37) and without LVH (G+/LVH−, n=29), patients with HCM without mutations (sarcomere-negative HCM, n=11), and healthy controls (n=11) underwent contrast cardiac magnetic resonance, measuring T1 times pre- and postgadolinium infusion. Concurrent echocardiography and serum biomarkers of collagen synthesis, hemodynamic stress, and myocardial injury were also available in a subset. Compared with controls, ECV was increased in patients with overt HCM, as well as G+/LVH− mutation carriers (ECV=0.36±0.01, 0.33±0.01, 0.27±0.01 in G+/LVH+, G+/LVH−, controls, respectively; $P \leq 0.001$ for all comparisons). ECV correlated with N-terminal probrain natriuretic peptide levels (r=0.58; $P<0.001$) and global E′ velocity (r=−0.48; $P<0.001$). Late gadolinium enhancement was present in >60% of overt patients with HCM but absent from G+/LVH− subjects. Both ECV and late gadolinium enhancement were more extensive in sarcomeric HCM than sarcomere-negative HCM.

Conclusions—Myocardial ECV is increased in HCM sarcomere mutation carriers even in the absence of LVH. These data provide additional support that fibrotic remodeling is triggered early in disease pathogenesis. Quantifying ECV may help characterize the development of myocardial fibrosis in HCM and ultimately assist in developing novel disease-modifying therapy, targeting interstitial fibrosis. (***Circ Cardiovasc Imaging***. 2013;6:415-422)

Key Words: fibrosis ■ gadolinium ■ genetics ■ hypertrophic cardiomyopathy ■ MRI

Hypertrophic cardiomyopathy (HCM) is caused by mutations in genes encoding sarcomere proteins.[1,2] The clinical diagnosis of HCM hinges on the presence of unexplained left ventricular hypertrophy (LVH). In contrast, genetic testing uniquely identifies family members with pathogenic sarcomere gene mutations (G+) who are at risk for developing HCM even when left ventricular (LV) wall thickness is normal (LVH−). By studying this subclinical genotype-positive, LVH-negative (G+/LVH−) population, early phenotypes of sarcomere mutations can be characterized, without the confounding influence of pathological changes that accompany overt disease. Impaired LV relaxation and altered myocardial energetics have been demonstrated in G+/LVH− subjects, indicating that sarcomere mutations cause primary cardiac abnormalities independently of LVH.[3–5]

Clinical Perspective on p 422

Myocardial fibrosis is a histopathologic hallmark of HCM, present as both dense replacement fibrosis (scar) and interstitial fibrosis. Fibrosis is presumed to play a role in important outcomes, such as sudden cardiac death, ventricular tachyarrhythmias, LV dysfunction, and heart failure.[6–10] However, the precise triggers that lead to the development of fibrosis are unknown. Transcriptional profiling performed in mouse models of HCM, genetically engineered to carry sarcomere mutations that cause human disease, have demonstrated that pathways involved in fibrosis and collagen deposition are activated early, before gross or histological LVH was detectable.[11] More recent human studies have shown that serum levels of carboxy-terminal propeptide of procollagen

© 2013 American Heart Association, Inc.

Circ Cardiovasc Imaging is available at http://circimaging.ahajournals.org   **DOI: 10.1161/CIRCIMAGING.112.000333**

type I (PICP), a biomarker of collagen type I synthesis, were increased in G+/LVH− subjects.[12] These studies suggest that a profibrotic milieu is present in the early stages of disease pathogenesis, when cardiac morphology seems normal.

Gadolinium-enhanced cardiac magnetic resonance (CMR) allows noninvasive visualization of extracellular volume (ECV) expansion and myocardial fibrosis.[13] Gadolinium diffuses into the interstitial space between cells but does not cross intact cell membranes. In scar, when the extracellular space is expanded (fibrosis, edema, infiltration), the volume of distribution of gadolinium is increased, resulting in accumulation, delayed clearance, and persistently higher concentrations of gadolinium relative to normal myocardium.[14,15] Late gadolinium enhancement (LGE) is visualized in >60% of patients with clinically overt HCM and likely represents dense replacement fibrosis.[8,16–23] However, there are important limitations of current LGE-based techniques, including the requirement to null the signal to a normal myocardial reference region.[13] In conditions such as HCM and aortic stenosis, fibrosis is diffuse and thus the reference myocardium is likely abnormal, leading to underestimation of the presence, severity, and extent of myocardial involvement.[24,25]

Techniques for measuring myocardial and blood T1 times or rates (R1=1/T1) before and after gadolinium administration have been applied to overcome limitations related to the binary detection of LGE. With these techniques, diffuse myocardial abnormalities, including interstitial fibrosis, can be quantified and are reflected by an increased volume of distribution of gadolinium. As illustrated in Figure 1, myocardial ECV can be robustly quantified by comparing changes in relaxation rates between pre- and postcontrast states in the myocardium relative to blood.[25–29] As such, these techniques provide a noninvasive means of assessing ECV expansion and diffuse myocardial fibrosis. T1 measurements have been validated against histological measures of myocardial collagen content in patients with aortic stenosis and HCM.[25] Shorter contrast-enhanced T1
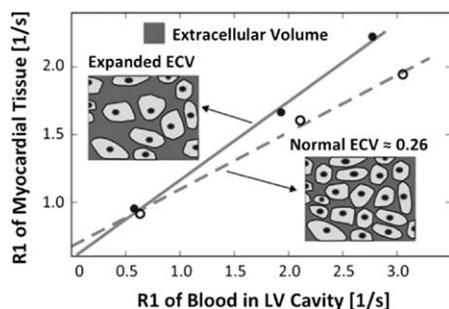

Figure 1. Estimating the myocardial extracellular volume (ECV) from T1 measurements. Cardiac magnetic resonance T1 measurements before and after gadolinium contrast administration are used to determine the change of the relaxation rate (R1=1/T1) in myocardial tissue relative to blood. Data are derived from the slope of a least squares linear regression that is fit to the measured R1 data. The slope corresponds to the partition coefficient for the extracellular gadolinium contrast in myocardial tissue. By multiplying the partition coefficient with 1-hematocrit, to adjust for the blood contrast volume of distribution, the ECV fraction of myocardial tissue can be estimated. An expansion of the extracellular space corresponds to an increase of the slope of the regression line. The figure insets illustrate the extracellular space and intact cardiac myocytes (from which gadolinium is excluded) in normal myocardium, and with expanded ECV. LV indicates left ventricle.

times may also identify subclinical myocardial dysfunction in patients with diabetes mellitus.[30] In this study, we aimed to test whether myocardial ECV is increased in sarcomere mutation carriers with overt HCM, as well as at-risk individuals without LVH. We also examined the pathophysiologic impact of ECV expansion by investigating their correlation with tissue Doppler echocardiography and serum biomarkers of collagen type I synthesis, myocardial injury, and hemodynamic stress.

Methods

Study Population

Written informed consent was obtained from all participants in protocols approved by the institutional review board of Brigham and Women's Hospital/Partners Healthcare, Boston, MA. Genotyped patients with HCM and relatives were identified via research protocols or clinical evaluation. Sarcomere mutations carriers (G+) had a pathogenic or presumed pathogenic HCM mutation, as defined by standard criteria.[4] Subjects were designated as having overt HCM (G+/LVH+) or subclinical HCM (G+/LVH−) based on echocardiographically determined LV wall thickness, as previously described.[12] The overt HCM cohort included sarcomere mutation carriers (G+) with a maximal LV wall thickness by ≥12 mm. The G+/LVH− HCM cohort consisted of sarcomere mutation carriers without LVH (maximal LV wall thickness <12 mm). More rigorous criteria were used to define study groups than routinely used to diagnose clinical HCM[31] to avoid including individuals with borderline LVH and emerging or mild cardiomyopathy in the G+/LVH− group. All G+/LVH− subjects were confirmed to have normal LV wall thickness by CMR.

Control subjects were healthy volunteers and relatives who did not carry a sarcomere mutation (G−/LVH−). Sarcomere-negative patients with HCM had a clinical diagnosis of HCM, based on echocardiographic evidence of unexplained LVH, but had negative genetic testing. In these subjects, direct DNA sequence analysis of 8 sarcomere genes (*MYH7, MYBPC3, TNNT2, TNNI3, TPM1, ACTC, MYL2, MYL3*), failed to identify a pathogenic or likely pathogenic mutation. Exclusion criteria included systemic hypertension (systolic blood pressure ≥140 or diastolic blood pressure ≥90 mmHg or on medical therapy), infiltrative or storage disease, coronary artery disease, valvular heart disease other than that associated with systolic anterior motion of the mitral valve, prior septal myectomy or alcohol septal ablation, presence of a permanent pacemaker or implantable cardioverter-defibrillator, contraindications to gadolinium administration, and atrial fibrillation.

Standard CMR Protocol

All image acquisitions were done with the subject in the supine position and using both EKG gating and breath-holding. All subjects were imaged on a 3.0-Tesla system (Tim Trio, Siemens, Erlangen, Germany). The standard protocol consisted of cine steady-state–free precession imaging (repetition time, 3.4 ms; echo time, 1.2 ms; in-plane spatial resolution, 1.6×2 mm; temporal resolution, 40–50 ms) for LV function and LV mass.[32] Cine imaging was obtained in 8 to 14 matching short-axis planes (8 mm thick with no gap) and 3 radial long-axis planes. For the calculation of LV mass and function, the endocardial and epicardial borders of the LV myocardium were manually traced on successive short-axis cine images at end-diastole and -systole. The papillary muscles were excluded in the LV mass calculation. LV mass was derived by the summation of discs method and multiplying the myocardial muscle volume by 1.05 g/cm and indexed to body surface area.[33] LV wall thickness was measured in ≥4 sections, anterior and posterior septal, lateral and inferior, in all subjects. The location and measurement of maximal LV wall thickness were also noted.

Late Gadolinium Enhancement

All patients underwent an LGE imaging protocol (time for repetition [TR], 4.8 ms; time to echo [TE], 1.3 ms; inversion time, 200–300 ms) to detect focal myocardial fibrosis. A segmented inversion-recovery

pulse sequence for LGE was used starting 10 to 15 minutes after cumulative 0.15 mmol/kg dose of gadolinium-diethylenetriamine pentaacetic acid (Bayer HealthCare Pharmaceuticals Inc, Wayne, NJ). LGE images were obtained in 8 to 14 matching short-axis (8 mm thick with no gap) and 3 radial long-axis planes. LGE was quantified using a semiautomated grayscale threshold technique using a cutoff of 6 SDs above the mean signal intensity.[24] The quantity of LGE was expressed in grams and as a percentage of the total LV myocardial mass. All LGE analyses were performed using commercially available software (QMassMR, version 7.4, Medis, Leiden, The Netherlands).

T1 Protocol and Analysis

T1 measurements were performed with a Look-Locker sequence (5,6) with a nonslice selective adiabatic inversion pulse, followed by segmented gradient-echo acquisition for 17 cardiac phases/times after inversion, spread over 2 cardiac cycles (temporal resolution, 80–100 ms precontrast and 45–55 ms postcontrast; slice thickness, 8 mm; TR>3 R-wave to R-wave (RR) intervals precontrast and 2 RR intervals postcontrast). The Look-Locker sequence was repeated in 3 parallel mid-LV short-axis slices (basal, mid, and distal), once before, and 3 to 5 additional times after the injection of gadolinium spanning a 30-minute period. For each Look-Locker sequence, the endocardial and epicardial borders of the 3 short-axis slices were traced and divided into the standard 16-segment model (QMassMR, version 7.4, Medis, Leiden, The Netherlands). The signal intensity versus time curves for each segment and the blood pool were used to determine segmental T1 through fitting to an analytic expression for the inversion recovery and correction for the radiofrequency pulse alteration of the inversion recovery.[34,35]

The accuracy of T1 measurements with the Look-Locker method was tested in Gd-doped phantoms, against the standard inversion-recovery spin-echo technique. The mean difference of R1 in 10 phantoms, using the Look-Locker and inversion recovery (IR) spin-echo techniques, was 0.069 s^{-1} (Bland–Altman 5% and 95% limits of agreement: −0.152 to 0.013), with the mean R1 covering a range from 0.36 to 6.7 s^{-1}. The intraclass correlation coefficient was 0.997 with a 95% confidence interval of 0.992 to 0.999.

T1 relaxation rate, calculated as the reciprocal of T1 (R1=1/T1), was used to plot the myocardial R1 against the R1 in the blood pool and calculate the slope by linear regression, using all measurement points with an R1 of <3 s^{-1}. The slope of the linear relationship defines the partition coefficient for gadolinium, λ_{Gd} (Figure 1). From the slope of this relationship, the myocardial ECV was obtained by multiplying each of the segmental λ_{Gd} by (1-hematocrit in percent/100) as reported previously.[28] An ECV fraction for each subject was then calculated by averaging the 16 myocardial segmental values from the 3 short-axis slices. Because of technical limitations in 18 subjects, a single representative mid-LV slice was used for analysis. In subjects with regional fibrosis detected by LGE, we also calculated a second ECV after excluding regions that contained LGE.

Echocardiographic Protocol

The Vivid-7 ultrasound system (GE Medical Systems, Milwaukee, WI) was used for standard echocardiography and tissue Doppler interrogation. Standard measures of cardiac dimensions and function from 2D spectral Doppler analysis were determined using the mean of 3 cardiac cycles, in accordance with guidelines of the American Society of Echocardiography.[36] Tissue Doppler myocardial velocities in early diastole (E') were measured at the lateral, septal, anterior, and inferior aspects of the mitral annulus in the apical 4- and 2-chamber views. Global values of E' were calculated as the average of these 4 measurements and reflect the velocity of early myocardial relaxation. Images were analyzed by 2 observers blinded to clinical and genetic status. Echocardiographic studies performed within 1 year of CMR imaging were included in this study.

Measurement of Serum Biomarkers

Blood samples (serum and K3-EDTA plasma) were available on an unselected subset of subjects who also participated in research protocols that included collection of blood for biomarker analysis. Samples were obtained at the time of cardiac imaging, processed within 60 minutes of phlebotomy, and stored at −80°C before analysis. All assays were performed using commercially available reagents by personnel who were blinded to clinical and genetic status. The following markers were analyzed: PICP (Quidel Corporation, San Diego, CA), amino terminal propeptide of B-type natriuretic peptide (NT-proBNP, Roche, Indianapolis, IN), and supersensitive cardiac troponin I (Singulex, Atlanta, GA).

Statistical Analysis

To test for differences between the 3 status groups or between patients with overt HCM with and without sarcomere mutations, ANOVA and logistic regression were performed with clustering to adjust for family relationships. An exchangeable correlation structure was assumed within families, except in one case where convergence issues required initial estimates based on independence, with correlation accounted for in the SEs in the final estimates. Age-dependent parameters of tissue Doppler, ECV, PICP, and N-terminal probrain natriuretic peptide (NT-proBNP) levels were adjusted for age, as well as family relationships; analyses were also adjusted for sex. Except where noted, values are expressed as adjusted mean±SE. For analyses across the 3 status groups (G+/LVH+, G+/LVH−, control), a P value <0.017 was considered statistically significant to apply post hoc Bonferroni correction for multiple comparisons. Pearson correlation was used to evaluate for associations between continuous measures. All analyses were performed with SAS version 9.2 (SAS Institute, Inc., Cary, NC).

Results

Clinical Characteristics

Eighty-eight individuals from 68 unrelated families were included in this study. These included 37 G+/LVH+ overt HCM subjects, 29 G+/LVH− subjects, 11 normal controls, and 11 sarcomere-negative HCM subjects. General clinical characteristics of sarcomere mutation carriers and normal controls are summarized in Table 1. Forty-eight different mutations in 6 sarcomere genes were represented, listed in the Table in the online-only Data Supplement: β-myosin heavy chain (*MYH7*, n=20), cardiac myosin binding protein C (*MYBPC3*, n=39), cardiac troponin T (*TNNT2*, n=5), cardiac troponin I (*TNNI3*, n=1), myosin essential light chain (*MYL2*, n=1), and myosin regulatory light chain (*MYL3*, n=1).

Echocardiographic studies were available in 76 subjects; 67% of studies were performed within 24 hours of CMR (median time difference, 0±73 days; range 0–349 days). Serum biomarker analysis was also available in 53 of these subjects (G+/LVH+, n=20; G+/LVH−, n=27; controls, n=6), and results are presented in Table 2. Serum PICP levels were significantly higher in G+/LVH+ and G+/LVH− subjects compared with healthy controls. Serum NT-proBNP levels were significantly higher in G+/LVH+ subjects compared with G+/LVH− and healthy controls. There were no significant differences in supersensitive cardiac troponin I levels across the cohorts.

T1 Measurement Results

Overall Cohort

CMR variables are presented in Table 2. Compared with normal controls, the ECV was increased in sarcomere mutation carriers, both with overt HCM and with normal LV wall thickness (Figure 2). There were significant correlations between ECV and serum NT-proBNP levels (Pearson r=0.54,

Table 1. Clinical Characteristics

	Control (n=11)	P Value (Control vs G+/LVH−)*	G+/LVH− (n=29)	P Value (G+/LVH− vs G+/LVH+)*	G+/LVH+ (n=37)	P Value (Control vs G+/LVH+)*
Age±SD (range), y	27.2±7.1(19–39)	0.50	28.1±9.5 (16–48)	<0.001	41.3±14.1 (19–73)	<0.001
Female (female/male), %	60 (6/4)	0.67	59 (17/12)	0.03	32 (12/25)	0.19
Causal gene, n						
MYH7			12		8	
MYBPC3			14		25	
TNNT2			3		2	
TNNI3			0		1	
MYL2			0		1	
MYL3			0		1	
BSA, m²	1.89±0.07	0.13	1.79±0.04	0.03	1.95±0.04	0.52
CMR maximal LV wall thickness, mm	7.8±0.4	0.54	8.1±0.4	<0.001	18.1±0.8	<0.001
CMR LV mass, g	106±8	0.20	96±7	<0.001	156±9	<0.001
CMR LV mass index, g/m²	52±5	0.63	49±3	<0.001	84±5	<0.001
CMR LVEDV, mL	175±11	0.06	154±7	0.30	164±6	0.49
CMR LVESV, mL	70±4	0.09	61±3	0.78	60±4	0.13
CMR LVEF, %	59±1	0.08	62±1	0.35	63±1	0.03

Data other than age are presented as means±SE, adjusted for family relations, sex, and age.

BSA indicates body surface area; CMR, cardiac magnetic resonance; LV, left ventricle; LVEDV, LV end-diastolic volume; LVEF, left ventricular ejection fraction; LVESV, LV end-systolic volume; and LVH, left ventricular hypertrophy.

*P values <0.017 are statistically significant and adjusted for age and family relations.

$P<0.001$ for NT-proBNP; $r=0.58$, $P<0.001$ for log NT-proBNP) and global E' velocity (Pearson $r=−0.48$, $P<0.001$), illustrated in Figure 3. There was a weak but significant correlation between ECV and myocardial mass (Pearson $r=0.36$, $P<0.001$). There was a weak correlation between LGE, but not ECV, and left ventricular ejection fraction (Pearson $r=−0.37$, $P<0.001$). No significant correlation was seen between ECV or LGE and serum PICP or supersensitive troponin levels. No obvious genotypic influence was detected. No significant differences in ECV were seen comparing *MYH7* and *MYBPC3* mutation carriers, with or without LVH (data not shown). For the overall cohort, the average precontrast T1 was ≈1087±81 ms (mean±SD) in myocardial segments and ≈1556±152 ms in the LV blood pool.

G+/LVH− Cohort

The mean age of G+/LVH− subjects was 28.1±9.5 years (range 16–48 years), and 59% were women. The myocardial ECV was 0.06 (22%) higher in G+/LVH− subjects (ECV=0.33±0.01) compared with controls (ECV=0.27±0.01; $P<0.001$; Table 2 and Figure 2). Despite increased ECV and serum PICP levels, LGE was not detected in any G+/LVH− subjects (Figure 4). Compared with normal controls, there were no significant differences in age, LV wall thickness, or LV mass. Subjects with *MYH7* mutations were younger than those with *MYBPC3* mutations (24.6 versus 31.9 years; $P=0.04$). *MYH7* mutation carriers also had significantly lower global E' velocity (13.2±0.7 versus 15.4±0.4 cm/sec; $P=0.003$).

Table 2. CMR Metrics of Fibrosis and Serum Biomarker Levels

	Control (n=11)	P Value (Control vs G+/LVH−)*	G+/LVH− (n=29)	P Value (G+/LVH− vs G+/LVH+)*	G+/LVH+ (n=37)	P Value (Control vs G+/LVH+)*
ECV (range)	0.27±0.01 (0.24–0.31)	<0.001	0.33±0.01 (0.23–0.38)	0.001	0.36±0.01 (0.31–0.51)	<0.001
LGE present (yes/no), %	0 (0/11)		0 (0/29)		78 (29/8)	
LGE±SD (range), g	0		0	0.004	15.6±25.8 (0.0–105.6)	0.003
LGE±SD (range), % LV mass	0		0	<0.001	7.4±10.4 (0.0–44.6%)	0.001
PICP, µg/L	69.3±4.1	<0.001	89.1±4.7	0.48	97.4±9.5	0.015
Singulex cTnI, pg/mL	3.1±1.5	0.38	6.0±3.7	0.24	14.2±5.5	0.09
NT-proBNP, pg/mL	52.9±52.0	0.24	81.3±44.5	0.002	325.8±79.2	0.002

LGE data are presented as unadjusted mean±SD. All other data are presented as means±SE, adjusted for family relations, sex, and age.

CMR indicates cardiac magnetic resonance; cTnI, cardiac troponin I; ECV, extracellular volume; LGE, late gadolinium enhancement; LV, left ventricle; LVH, left ventricular hypertrophy; PICP, carboxy-terminal propeptide of procollagen type I; and NT-proBNP, N-terminal probrain of B-type natriuretic peptide.

*P values <0.017 are statistically significant and adjusted for age and family relations.
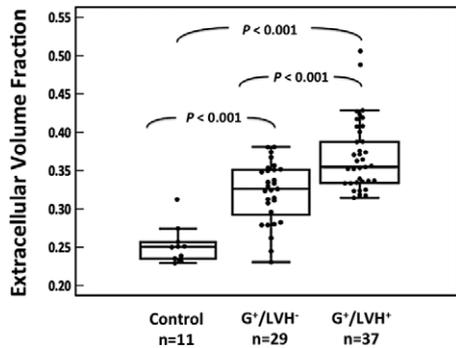
Figure 2. The myocardial extracellular volume (ECV) is significantly increased in hypertrophic cardiomyopathy (HCM) sarcomere mutation carriers with and without left ventricular hypertrophy (LVH). Compared with normal controls, ECV was 22% higher in G+/LVH− subjects and 33% higher in patients with G+/LVH+ HCM. ECV in overt HCM subjects was 9% higher than G+/LVH− subjects (*P*≤0.001 for all comparisons).

Overt HCM Cohort

The mean age of G+/LVH+ patients was 41.3±14.1 years (range 19–73 years), and 32% were women. The myocardial ECV was highest in this subgroup, even after excluding segments with LGE in subjects with overt HCM. In G+/LVH+ subjects, ECV measured was 0.36±0.01; 0.09 (33%) higher

Figure 3. The myocardial extracellular volume (ECV) is correlated to serum N-terminal probrain natriuretic peptide (NT-proBNP) levels and E' velocity. **A**, ECV was significantly positively correlated to serum NT-proBNP levels in the overall cohort excluding patients with sarcomere-negative hypertrophic cardiomyopathy (serum biomarkers not available for this cohort). **B**, ECV was significantly inversely correlated echocardiographic global E' velocities in the overall cohort.

than controls, and 0.03 (9%) higher than G+/LVH− subjects (*P*≤0.001 for all comparisons; Table 2 and Figure 2). LGE was present in 78% of sarcomere mutation carriers with overt HCM (Table 2 and Figure 4). Age, LV wall thickness, and LV mass were significantly higher in G+/LVH+ subjects compared with G+/LVH− subjects and normal controls.

G+/LVH+ patients with sarcomeric HCM were compared with patients with sarcomere-negative HCM. Results are summarized in Table 3. Patients with sarcomeric HCM had more pronounced abnormalities in CMR metrics of myocardial fibrosis than patients with HCM without sarcomere mutations. Although there was no significant difference in the prevalence of LGE, the extent was greater in patients with sarcomere mutations. ECV was also higher in patients with sarcomeric HCM, even after excluding segments with LGE. There was a strong correlation between ECV and the extent of LGE (Pearson *r*=0.76; *P*<0.001), and a weak correlation between both ECV and LGE and left ventricular ejection fraction (Pearson *r*=−0.42 to −0.5; *P*≤0.003).

Discussion

We report evidence of abnormal ECV expansion in HCM. Cardiac MRI with pre- and postcontrast T1 measurements demonstrated a significant increase in myocardial ECV not only in patients with clinically overt disease, but also notably in sarcomere mutation carriers with normal LV wall thickness. These results suggest that HCM sarcomere mutations lead to myocardial abnormalities, potentially reflecting increased interstitial fibrosis, independently of LVH. These findings are an important advance from LGE methodology that identifies dense, focal scar but cannot capture more diffuse expansion of the extracellular space, such as caused by interstitial fibrosis, edema, inflammation, or infiltrative processes. Indeed, myocardial ECV seems to be more discriminating for the presence of a sarcomere mutation than LGE because LGE is very rarely seen in mutation carriers before the development of LVH and was not present in our cohort of G+/LVH− subjects (Figure 4).

We have postulated that myocardial fibrosis is a fundamental and early consequence of sarcomere mutations rather than simply a downstream response to the LVH, outflow obstruction, and ischemia associated with clinically overt HCM.[12] This hypothesis was initially based on unbiased transcriptional profiling in a mouse model of HCM. These studies demonstrated that young animals with sarcomere mutations had significant and early upregulation of genes involved in extracellular matrix formation.[11] Genetic pathways were activated well before histological or gross LVH or fibrosis developed. More recent human studies similarly indicated that myocardial type I collagen synthesis is increased in sarcomere mutation carriers, in the absence of LVH or LGE.[12] We now describe expansion of myocardial ECV in the at-risk G+/LVH− population. Although the pathways have not yet been characterized, collectively these findings suggest that sarcomere gene mutations drive a profibrotic state early in disease pathogenesis.

We also explored the potential functional and pathophysiological impact of increased myocardial ECV. There was a significant positive correlation between ECV and serum NT-proBNP levels, and a significant negative correlation
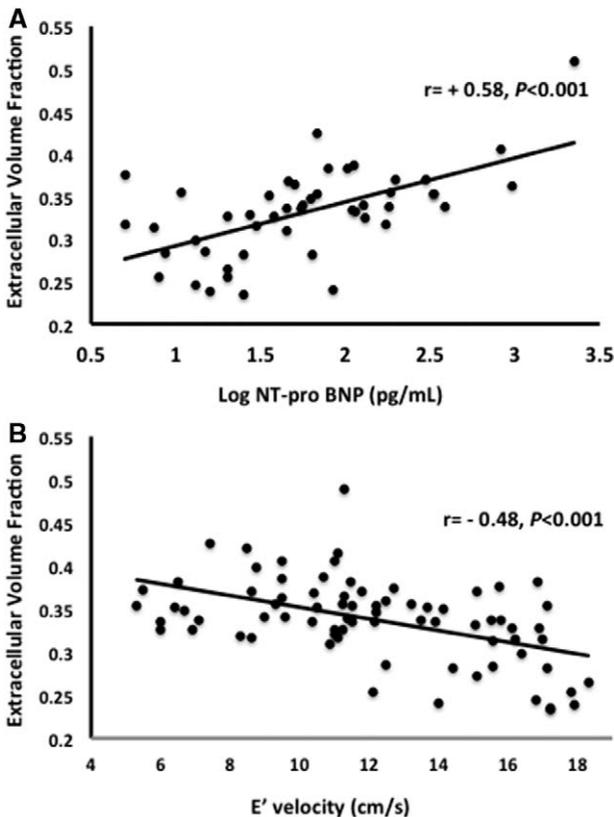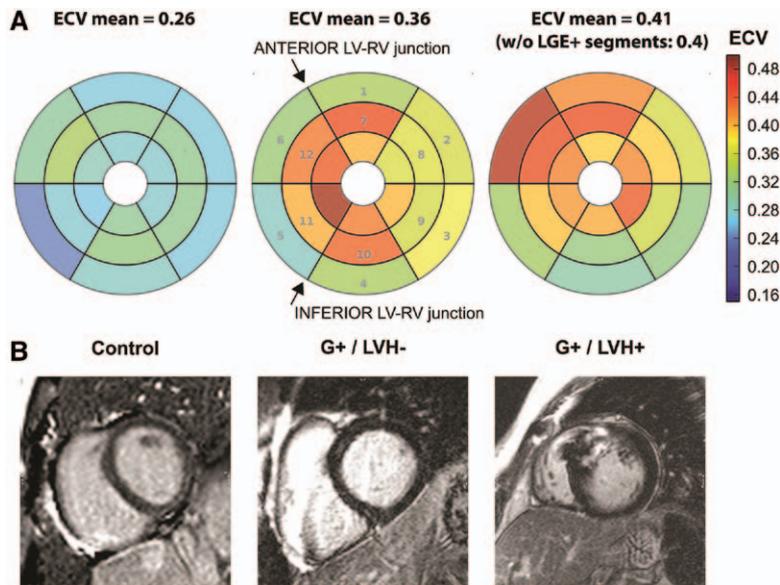
Figure 4. Graphic comparison of T1 measurements and late gadolinium enhancement (LGE). **A**, Bull's eye representation of results from segmental analysis (numbers correspond to American Heart Association segment numbering for basal and mid-level slices) of T1 measurements before and after gadolinium contrast administration. Compared with healthy controls (images on **left**), the myocardial extracellular volume (ECV) was elevated in sarcomere mutation carriers (G+), both in the absence (**middle**) or presence (**right**) of left ventricular hypertrophy (LVH). In the G+/LVH+ subject, the ECV remained highly abnormal if LGE+ segments were excluded. **B**, Representative LGE images from the same subjects, in midlevel locations corresponding to one of the levels for the T1 measurements of ECV. LGE is not seen in the normal control or the G+/LVH− subject, despite significantly increased ECV in the latter. The G+/LVH+ subject with overt hypertrophic cardiomyopathy demonstrates prominent LGE near the anterior left venticular (LV)/right ventricular (RV) junction.

between ECV and global E' velocities. These observations are consistent with the theory that ECV expansion results in diastolic dysfunction. These changes may contribute to the reduced E' velocities seen in G+/LVH− mutation carriers.[3,4]

Our findings also indicate that the fibrotic burden is higher in patients with HCM with sarcomere mutations compared with those without a sarcomere mutation. Both LGE and ECV were significantly more extensive in sarcomeric HCM. These results may partly underlie the worse outcomes reported in sarcomere-positive versus sarcomere-negative HCM, where an increased risk of cardiovascular death, nonfatal stroke, or worsening New York Heart Association functional class was observed in patients with sarcomere mutations.[37]

Important limitations of this study are the relatively small population and the cross-sectional design, measuring T1 values in 2 distinct stages of HCM: G+/LVH− and G+/LVH+. Moreover, T1 quantification of ECV is not specific for myocardial fibrosis. Myocardial edema, inflammation,

infiltrative processes, and increased sarcolemmal permeability will also lead to increased ECV. In this study, there was no significant positive correlation between ECV and serum PICP levels, a biomarker of collagen synthesis. Comprehensive and longitudinal studies in larger populations, anchored by genotype, are needed to better define the processes that truly underlie abnormalities of serum biomarkers, altered myocardial gadolinium distribution, and myocardial fibrosis in the pathogenesis of HCM. Such critical studies will also allow assessment of their impact on key disease manifestations, such as the development of arrhythmias and heart failure.

CMR T1 measurement is another tool to study disease biology, identifying and quantifying myocardial ECV expansion. Previous reports have demonstrated abnormal expansion of the extracellular space using precontrast T1 mapping methods,[38] as well as pre- and postcontrast T1 mapping methods[39–41] in patients with phenotypically established HCM and LVH. In this report, we extend this experience to at-risk individuals

Table 3. Comparison of Patients With Clinically Overt HCM With and Without Sarcomere Mutations

	Sarcomere (+) HCM (n=37)	Sarcomere (−) HCM (n=11)	P Value*
Age±SD (range), y	41.3±14.1 (19–73)	44.6±11.1 (25–63)	0.29
Female (female/male), %	32 (12/25)	9 (1/10)	0.17
BSA, m^2	1.93±0.04	2.21±0.06	<0.0001
Maximal LV wall thickness, mm	18.6±0.8	17.7±1.2	0.54
LV mass, g	169±12	200±15	0.11
LV mass index, g/m^2	87±5	91±7	0.65
LVEF, %	62±1	69±2	0.01
ECV	0.37±0.01	0.35±0.01	0.03
ECV, excluding LGE	0.37±0.00	0.34±0.01	0.04
LGE present (yes/no), %	78 (29/8)	64 (7/4)	0.35
LGE, g	15.9±4.2	4.3±2.2	0.02
LGE, % LV mass	18.2±0.04	5.2±3.7	<0.001

Data are presented as means±SE, adjusted for family relations and age.

BSA indicates body surface area; ECV, extracellular volume; HCM, hypertrophic cardiomyopathy; LGE, late gadolinium enhancement; LV, left ventricle and LVEF, left ventricular ejection fraction.

*P values <0.05 are statistically significant and adjusted for age and family relations.

without overt LVH to test the hypothesis that expansion of the extracellular space precedes the development of gross structural changes. Along with diastolic dysfunction,[3,4] impaired energetics,[5] and increased collagen synthesis,[12] these findings of myocardial ECV expansion provide more evidence that sarcomere gene mutations detrimentally impact the heart before the development of LVH. A profibrotic state seems to be a fundamental feature of HCM and an early phenotype of sarcomere mutations. This profibrotic milieu may contribute importantly to diastolic abnormalities and adverse clinical outcomes in HCM. However, in contrast to dense scar, formation of interstitial fibrosis may be a more dynamic and reversible process.[42–44] As such, monitoring ECV could provide a means of following disease progression as well as response to future, disease-modifying therapy. Developing treatments targeted at interstitial fibrosis may have the potential to change the pathophysiologic substrate, thereby diminishing disease progression and reducing the risk of arrhythmias and heart failure in HCM.

Disclosures

References

1. Seidman JG, Seidman C. The genetic basis for cardiomyopathy: from mutation identification to mechanistic paradigms. *Cell*. 2001;104:557–567.
2. Richard P, Villard E, Charron P, Isnard R. The genetic bases of cardiomyopathies. *J Am Coll Cardiol*. 2006;48:A79–A89.
3. Ho CY, Sweitzer NK, McDonough B, Maron BJ, Casey SA, Seidman JG, Seidman CE, Solomon SD. Assessment of diastolic function with Doppler tissue imaging to predict genotype in preclinical hypertrophic cardiomyopathy. *Circulation*. 2002;105:2992–2997.
4. Ho CY, Carlsen C, Thune JJ, Havndrup O, Bundgaard H, Farrohi F, Rivero J, Cirino AL, Andersen PS, Christiansen M, Maron BJ, Orav EJ, Køber L. Echocardiographic strain imaging to assess early and late consequences of sarcomere mutations in hypertrophic cardiomyopathy. *Circ Cardiovasc Genet*. 2009;2:314–321.
5. Crilley JG, Boehm EA, Blair E, Rajagopalan B, Blamire AM, Styles P, McKenna WJ, Ostman-Smith I, Clarke K, Watkins H. Hypertrophic cardiomyopathy due to sarcomeric gene mutations is characterized by impaired energy metabolism irrespective of the degree of hypertrophy. *J Am Coll Cardiol*. 2003;41:1776–1782.
6. Basso C, Thiene G, Corrado D, Buja G, Melacini P, Nava A. Hypertrophic cardiomyopathy and sudden death in the young: pathologic evidence of myocardial ischemia. *Hum Pathol*. 2000;31:988–998.
7. Shirani J, Pick R, Roberts WC, Maron BJ. Morphology and significance of the left ventricular collagen network in young patients with hypertrophic cardiomyopathy and sudden cardiac death. *J Am Coll Cardiol*. 2000;35:36–44.
8. Choudhury L, Mahrholdt H, Wagner A, Choi KM, Elliott MD, Klocke FJ, Bonow RO, Judd RM, Kim RJ. Myocardial scarring in asymptomatic or mildly symptomatic patients with hypertrophic cardiomyopathy. *J Am Coll Cardiol*. 2002;40:2156–2164.
9. Varnava AM, Elliott PM, Mahon N, Davies MJ, McKenna WJ. Relation between myocyte disarray and outcome in hypertrophic cardiomyopathy. *Am J Cardiol*. 2001;88:275–279.
10. Varnava AM, Elliott PM, Sharma S, McKenna WJ, Davies MJ. Hypertrophic cardiomyopathy: the interrelation of disarray, fibrosis, and small vessel disease. *Heart*. 2000;84:476–482.
11. Kim JB, Porreca GJ, Song L, Greenway SC, Gorham JM, Church GM, Seidman CE, Seidman JG. Polony multiplex analysis of gene expression (PMAGE) in mouse hypertrophic cardiomyopathy. *Science*. 2007;316:1481–1484.
12. Ho CY, López B, Coelho-Filho OR, Lakdawala NK, Cirino AL, Jarolim P, Kwong R, González A, Colan SD, Seidman JG, Díez J, Seidman CE. Myocardial fibrosis as an early manifestation of hypertrophic cardiomyopathy. *N Engl J Med*. 2010;363:552–563.
13. Kim RJ, Fieno DS, Parrish TB, Harris K, Chen EL, Simonetti O, Bundy J, Finn JP, Klocke FJ, Judd RM. Relationship of MRI delayed contrast enhancement to irreversible injury, infarct age, and contractile function. *Circulation*. 1999;100:1992–2002.
14. Flacke SJ, Fischer SE, Lorenz CH. Measurement of the gadopentetate dimeglumine partition coefficient in human myocardium in vivo: normal distribution and elevation in acute and chronic infarction. *Radiology*. 2001;218:703–710.
15. Kim RJ, Chen EL, Lima JA, Judd RM. Myocardial Gd-DTPA kinetics determine MRI contrast enhancement and reflect the extent and severity of myocardial injury after acute reperfused infarction. *Circulation*. 1996;94:3318–3326.
16. Moon JC, McKenna WJ, McCrohon JA, Elliott PM, Smith GC, Pennell DJ. Toward clinical risk assessment in hypertrophic cardiomyopathy with gadolinium cardiovascular magnetic resonance. *J Am Coll Cardiol*. 2003;41:1561–1567.
17. Moon JC, Mogensen J, Elliott PM, Smith GC, Elkington AG, Prasad SK, Pennell DJ, McKenna WJ. Myocardial late gadolinium enhancement cardiovascular magnetic resonance in hypertrophic cardiomyopathy caused by mutations in troponin I. *Heart*. 2005;91:1036–1040.
18. Adabag AS, Maron BJ, Appelbaum E, Harrigan CJ, Buros JL, Gibson CM, Lesser JR, Hanna CA, Udelson JE, Manning WJ, Maron MS. Occurrence and frequency of arrhythmias in hypertrophic cardiomyopathy in relation to delayed enhancement on cardiovascular magnetic resonance. *J Am Coll Cardiol*. 2008;51:1369–1374.
19. Maron MS, Appelbaum E, Harrigan CJ, Buros J, Gibson CM, Hanna C, Lesser JR, Udelson JE, Manning WJ, Maron BJ. Clinical profile and significance of delayed enhancement in hypertrophic cardiomyopathy. *Circ Heart Fail*. 2008;1:184–191.
20. Rudolph A, Abdel-Aty H, Bohl S, Boyé P, Zagrosek A, Dietz R, Schulz-Menger J. Noninvasive detection of fibrosis applying contrast-enhanced cardiac magnetic resonance in different forms of left ventricular hypertrophy relation to remodeling. *J Am Coll Cardiol*. 2009;53:284–291.
21. Bruder O, Wagner A, Jensen CJ, Schneider S, Ong P, Kispert EM, Nassenstein K, Schlosser T, Sabin GV, Sechtem U, Mahrholdt H. Myocardial scar visualized by cardiovascular magnetic resonance imaging predicts major adverse events in patients with hypertrophic cardiomyopathy. *J Am Coll Cardiol*. 2010;56:875–887.
22. O'Hanlon R, Grasso A, Roughton M, Moon JC, Clark S, Wage R, Webb J, Kulkarni M, Dawson D, Sulaibeekh L, Chandrasekaran B, Bucciarelli-Ducci C, Pasquale F, Cowie MR, McKenna WJ, Sheppard MN, Elliott PM, Pennell DJ, Prasad SK. Prognostic significance of myocardial fibrosis in hypertrophic cardiomyopathy. *J Am Coll Cardiol*. 2010;56:867–874.
23. Rubinshtein R, Glockner JF, Ommen SR, Araoz PA, Ackerman MJ, Sorajja P, Bos JM, Tajik AJ, Valeti US, Nishimura RA, Gersh BJ. Characteristics and clinical significance of late gadolinium enhancement by contrast-enhanced magnetic resonance imaging in patients with hypertrophic cardiomyopathy. *Circ Heart Fail*. 2010;3:51–58.
24. Flett AS, Hasleton J, Cook C, Hausenloy D, Quarta G, Ariti C, Muthurangu V, Moon JC. Evaluation of techniques for the quantification of myocardial scar of differing etiology using cardiac magnetic resonance. *J Am Coll Cardiol Cardiovasc Imaging*. 2011;4:150–156.
25. Flett AS, Hayward MP, Ashworth MT, Hansen MS, Taylor AM, Elliott PM, McGregor C, Moon JC. Equilibrium contrast cardiovascular magnetic resonance for the measurement of diffuse myocardial fibrosis: preliminary validation in humans. *Circulation*. 2010;122:138–144.
26. Jerosch-Herold M, Sheridan DC, Kushner JD, Nauman D, Burgess D, Dutton D, Alharethi R, Li D, Hershberger RE. Cardiac magnetic resonance imaging of myocardial contrast uptake and blood flow in patients affected with idiopathic or familial dilated cardiomyopathy. *Am J Physiol Heart Circ Physiol*. 2008;295:H1234–H1242.
27. Iles L, Pfluger H, Phrommintikul A, Cherayath J, Aksit P, Gupta SN, Kaye DM, Taylor AJ. Evaluation of diffuse myocardial fibrosis in heart failure with cardiac magnetic resonance contrast-enhanced T1 mapping. *J Am Coll Cardiol*. 2008;52:1574–1580.
28. Broberg CS, Chugh SS, Conklin C, Sahn DJ, Jerosch-Herold M. Quantification of diffuse myocardial fibrosis and its association with

myocardial dysfunction in congenital heart disease. *Circ Cardiovasc Imaging*. 2010;3:727–734.

29. Ugander M, Oki AJ, Hsu LY, Kellman P, Greiser A, Aletras AH, Sibley CT, Chen MY, Bandettini WP, Arai AE. Extracellular volume imaging by magnetic resonance imaging provides insights into overt and sub-clinical myocardial pathology. *Eur Heart J*. 2012;33:1268–1278.

30. Ng AC, Auger D, Delgado V, van Elderen SG, Bertini M, Siebelink HM, van der Geest RJ, Bonetti C, van der Velde ET, de Roos A, Smit JW, Leung DY, Bax JJ, Lamb HJ. Association between diffuse myocardial fibrosis by cardiac magnetic resonance contrast-enhanced T_1 mapping and subclinical myocardial dysfunction in diabetic patients: a pilot study. *Circ Cardiovasc Imaging*. 2012;5:51–59.

31. McKenna WJ, Spirito P, Desnos M, Dubourg O, Komajda M. Experience from clinical genetics in hypertrophic cardiomyopathy: proposal for new diagnostic criteria in adult members of affected families. *Heart*. 1997;77:130–132.

32. Steel K, Broderick R, Gandla V, Larose E, Resnic F, Jerosch-Herold M, Brown KA, Kwong RY. Complementary prognostic values of stress myocardial perfusion and late gadolinium enhancement imaging by cardiac magnetic resonance in patients with known or suspected coronary artery disease. *Circulation*. 2009;120:1390–1400.

33. Grothues F, Smith GC, Moon JC, Bellenger NG, Collins P, Klein HU, Pennell DJ. Comparison of interstudy reproducibility of cardiovascular magnetic resonance with two-dimensional echocardiography in normal subjects and in patients with heart failure or left ventricular hypertrophy. *Am J Cardiol*. 2002;90:29–34.

34. Deichmann R, Hahn D, Haase A. Fast T1 mapping on a whole-body scanner. *Magn Reson Med*. 1999;42:206–209.

35. Messroghli DR, Rudolph A, Abdel-Aty H, Wassmuth R, Kühne T, Dietz R, Schulz-Menger J. An open-source software tool for the generation of relaxation time maps in magnetic resonance imaging. *BMC Med Imaging*. 2010;10:16.

36. Lang RM, Bierig M, Devereux RB, Flachskampf FA, Foster E, Pellikka PA, Picard MH, Roman MJ, Seward J, Shanewise JS, Solomon SD, Spencer KT, Sutton MS, Stewart WJ. Recommendations for chamber quantification: a report from the American Society of Echocardiography's Guidelines and Standards Committee and the Chamber Quantification Writing Group, developed in conjunction with the European Association of Echocardiography, a branch of the European Society of Cardiology. *J Am Soc Echocardiogr*. 2005;18:1440–1463.

37. Olivotto I, Girolami F, Ackerman MJ, Nistri S, Bos JM, Zachara E, Ommen SR, Theis JL, Vaubel RA, Re F, Armentano C, Poggesi C, Torricelli F, Cecchi F. Myofilament protein gene mutation screening and outcome of patients with hypertrophic cardiomyopathy. *Mayo Clin Proc*. 2008;83:630–638.

38. Dass S, Suttie JJ, Piechnik SK, Ferreira VM, Holloway CJ, Banerjee R, Mahmod M, Cochlin L, Karamitsos TD, Robson MD, Watkins H, Neubauer S. Myocardial tissue characterization using magnetic resonance noncontrast T1 mapping in hypertrophic and dilated cardiomyopathy. *Circ Cardiovasc Imaging*. 2012;5:726–733.

39. Amano Y, Takayama M, Kumita S. Contrast-enhanced myocardial T1-weighted scout (Look-Locker) imaging for the detection of myocardial damages in hypertrophic cardiomyopathy. *J Magn Reson Imaging*. 2009;30:778–784.

40. Ellims AH, Iles LM, Ling LH, Hare JL, Kaye DM, Taylor AJ. Diffuse myocardial fibrosis in hypertrophic cardiomyopathy can be identified by cardiovascular magnetic resonance, and is associated with left ventricular diastolic dysfunction. *J Cardiovasc Magn Reson*. 2012;14:76.

41. Kellman P, Wilson JR, Xue H, Bandettini WP, Shanbhag SM, Druey KM, Ugander M, Arai AE. Extracellular volume fraction mapping in the myocardium, part 2: initial clinical experience. *J Cardiovasc Magn Reson*. 2012;14:64.

42. Zannad F, Alla F, Dousset B, Perez A, Pitt B. Limitation of excessive extracellular matrix turnover may contribute to survival benefit of spironolactone therapy in patients with congestive heart failure: insights from the Randomized Aldactone Evaluation Study (RALES). Rales Investigators. *Circulation*. 2000;102:2700–2706.

43. Díez J, Querejeta R, López B, González A, Larman M, Martínez Ubago JL. Losartan-dependent regression of myocardial fibrosis is associated with reduction of left ventricular chamber stiffness in hypertensive patients. *Circulation*. 2002;105:2512–2517.

44. López B, Querejeta R, González A, Sánchez E, Larman M, Díez J. Effects of loop diuretics on myocardial fibrosis and collagen type I turnover in chronic heart failure. *J Am Coll Cardiol*. 2004;43:2028–2035.

CLINICAL PERSPECTIVE

Hypertrophic cardiomyopathy (HCM) is caused by mutations in sarcomere genes. Increased myocardial fibrosis is a histopathologic hallmark of HCM and thought to contribute to important outcomes, such as sudden cardiac death, ventricular tachyarrhythmias, and heart failure. However, the triggers that lead to the development of fibrosis. Animal and human investigations suggest that a profibrotic milieu is present early in disease pathogenesis, even when cardiac morphology seems normal. In this study, we measured T1 times by cardiac MRI to characterize extracellular volume (ECV) expansion in HCM and to test the hypothesis that expansion of the extracellular space precedes the development of cardiac hypertrophy. We found that myocardial ECV was significantly increased not only in patients with clinically overt disease, but also in at-risk mutation carriers with normal left ventricle wall thickness. We also explored the potential functional impact of increased ECV. There was a significant positive correlation between ECV and serum amino- terminal propeptide of B-type natriuretic peptide (NT-proBNP) levels, and a negative correlation between ECV and global E' velocities, suggesting that increased ECV impairs left ventricle filling. Along with diastolic dysfunction, altered energetics, and increased collagen synthesis, these findings of myocardial ECV expansion provide more evidence that sarcomere gene mutations detrimentally impact the heart before gross structural changes develop. A profibrotic state seems to be a fundamental, early phenotype of sarcomere mutations and may contribute to diastolic abnormalities and adverse clinical outcomes in HCM. Developing treatments to reduce interstitial fibrosis may diminish disease progression and decrease the risk of arrhythmias and heart failure in HCM.

Circulation

Cardiovascular Imaging

American Heart Association®

T1 Measurements Identify Extracellular Volume Expansion in Hypertrophic Cardiomyopathy Sarcomere Mutation Carriers With and Without Left Ventricular Hypertrophy

Carolyn Y. Ho, Siddique A. Abbasi, Tomas G. Neilan, Ravi V. Shah, Yucheng Chen, Bobak Heydari, Allison L. Cirino, Neal K. Lakdawala, E. John Orav, Arantxa González, Begoña López, Javier Díez, Michael Jerosch-Herold and Raymond Y. Kwong

The online version of this article, along with updated information and services, is located on the
World Wide Web at:
http://circimaging.ahajournals.org/content/6/3/415

Data Supplement (unedited) at:
http://circimaging.ahajournals.org/content/suppl/2013/04/02/CIRCIMAGING.112.000333.DC1

Supplemental Material

Supplemental Table. Sarcomere mutations present in the study cohort.

Gene	Mutation	# of Families	# of Subjects
MYH7 (n=20)	Ala797Thr	1	2
	Arg249Gln	1	1
	Arg858Gly	1	1
	Glu497Asp	1	1
	Gly584Arg	1	1
	Gly768Arg	1	1
	Lys847del	1	1
	Arg663Cys	2	2
	Val338Met	1	1
	Val39Met	1	2
	Ser291Phe	1	2
	Arg249Gln	1	1
	Arg870His	1	1
	Arg652Gly	1	1
	Arg453Cys	1	1
	Val1459Asn	1	1
MYBPC3 (n=39)	927-9G>A	1	2
	Val771Ala	1	1
	Leu1014fs	1	1
	Arg502Gln	2	2
	Gly531Arg	1	1
	3190+1 G>A	2	2
	Gln969X	1	2
	Trp1112Stop	1	1
	Ser858Asn	1	2
	927-9G>A	3	3
	Phe1246fs	1	1
	3190+2T>G	1	1
	Arg810His	1	1
	Pro1208fs	1	1
	Glu258Lys	2	4
	Arg502Trp	2	2
	Pro699fs	1	1
	Gly1248_Cys1253dup	1	1
	K1209fs	1	1
	Asp7Asn	1	1
	Gly531Arg	1	1
	1298-2A>G	1	1
	Asp770Asn	1	1
	Pro955fs	1	1
	Gln60fs	1	1
	Asp605Asn	1	1
	Arg943X	1	1
TNNT2 (n=5)	Arg92Trp	1	2
	Arg278Cys	1	3
TNNI3	Asp196Asn	1	1

(n=1)			
MYL2 (n=1)	Glu65Lys	1	1
MYL3 (n=1)	Val156Met	1	1